NEA/NSC/DOC/(95)03/IV
Volume IV

LEU-SOL-THERM-003

FULL AND TRUNCATED BARE SPHERES OF 10% ENRICHED URANYL NITRATE WATER SOLUTIONS

Evaluators

Anatoli Tsiboulia
Yevgeniy Rozhikhin
Victor Gurin
Institute of Physics and Power Engineering

Internal Reviewer
Mark Nikolaev

Independent Reviewer

Virginia F. Dean
Consultant to Idaho National Engineering Laboratory

FULL AND TRUNCATED BARE SPHERES OF 10% ENRICHED URANYL NITRATE WATER SOLUTIONS

SPECTRA

IDENTIFICATION NUMBER: LEU-SOL-THERM-003

KEY WORDS: acceptable, bare, critical experiment, homogeneous, low enriched, sphere, unreflected, uranium, uranyl nitrate, solution, water solution

1.0 DETAILED DESCRIPTION

1.1 Overview of Experiment

A series of critical experiments with aqueous uranyl nitrate solutions with uranium enriched to 10 wt.% ^{235}U was performed in 1965 at the Solution Critical Facility of the Institute of Physics and Power Engineering, Obninsk, Russia. Critical experiment measurements were made with solution in thin-wall spherical tanks without reflectors. Spheres with outer diameters of 66 cm, 88 cm, and 120 cm were used. Criticality was achieved at two partial fillings of each sphere and at full fillings (nine critical states). One experiment differed from another in geometry size and in uranium concentration in the solution. Descriptions of the experiments are given in References 1 and 2. Some details of the experiments were found by the experimenters in their workbooks.

All nine experiments presented here are considered to be acceptable for use as benchmark experiments.

1.2 Description of Experimental Configuration

A diagram of the critical assemblies is shown in Figure 1 (vertical cut). The experiments were performed in a room with dimensions 7.5 × 5.5 × 8.8 m high. The arrangement of the assemblies in the room is shown in Figure 2 (view from above).

The spherical tanks of the assemblies were located nearly equidistant from the three nearest concrete walls, which were 100 cm thick, at a distance of about 6.3 m from the concrete ceiling, which was 75 cm thick, and at a distance of about 1.3 - 1.8 m from the concrete floor, which was 20 cm thick. The walls and floor were lined with stainless steel 3 mm thick up to a height of 284 cm. The doorways shown in Figure 2 were closed by sliding concrete and steel doors (50 cm of concrete lined with 5 cm of steel). In Figure 1 a cylindrical stainless steel tank (diameter - 200 cm, height - 120 cm, wall thickness - 4 mm) sitting on the floor is shown. It was empty in this series of experiments. The sphere was fastened at the top to a special steel platform (150 × 150 × 1.5 cm thick) by a 50-cm-long rectangular neck and by four steel ropes 0.4 cm in diameter. The neck cross section (outer dimensions) was 4 × 10 cm, and its wall thickness was 0.5 cm. The neck was attached to the platform by a 1-cm-thick flange 30 cm in diameter. The four steel ropes were welded to a steel belt (a rod

1.2 cm in diameter) which girdled the sphere 5 cm below its equator. The platform was supported by steel channels.

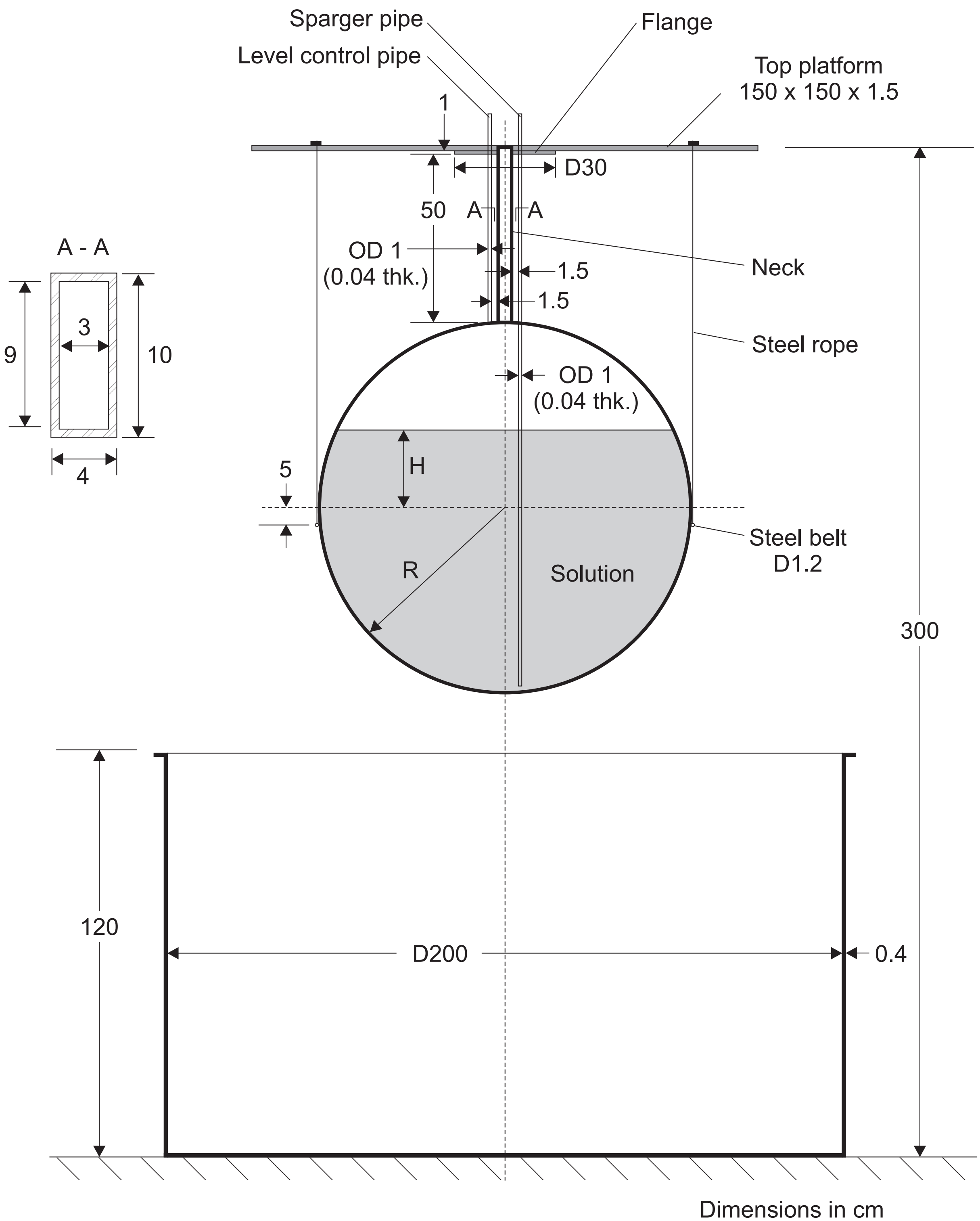

Figure 1. Vertical Cut of the Critical Assembly.

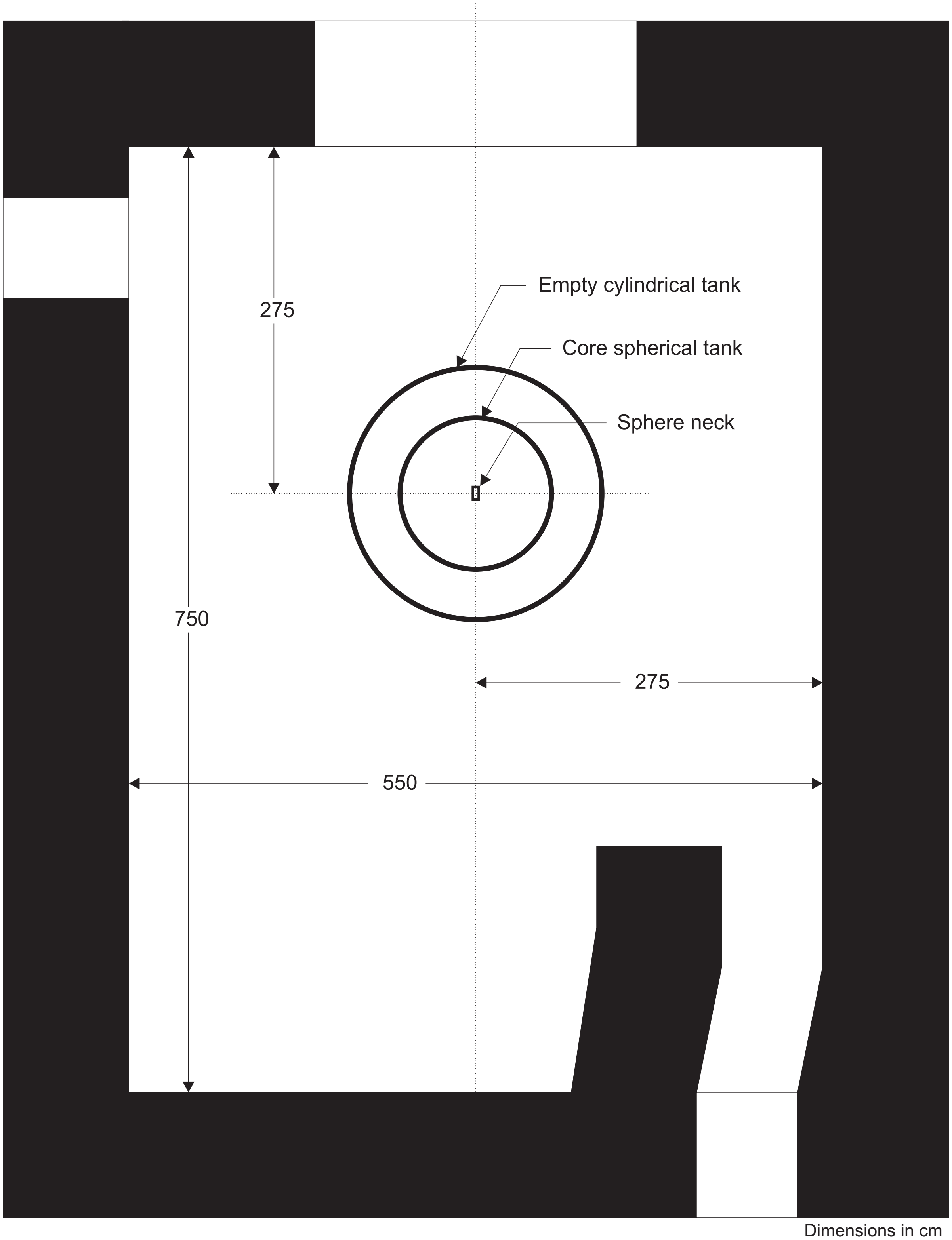

Figure 2. Arrangement of Critical Assembly in the Room (view from above).
(Distances are given in cm.)

Two control rods and one safety rod were used in a control and safety system. The control rods were stainless steel tubes with outer diameter 25 mm and wall thickness 2 mm filled with a powder of natural boron carbide with density 1.25 g/cm^3. The safety rod was rectangular cadmium plate with width 20 mm, 2 mm thick, and 600 mm high in a stainless steel clad with thickness 0.5 mm. All rods moved in vertical stainless steel guide tubes which were 60 cm from the sphere surface. The outer diameter of the guide tubes for the control rods was 30 mm with wall thickness 2 mm. The outer dimensions of the guide tube for the safety rod were 14×29 mm with wall thickness 2 mm. The lower ends of the control and safety rods in their upper positions were about 15 cm above the level of the top of the sphere.

A neutron source was placed near the surface of the sphere in the process of achievement of criticality, but critical conditions were determined with the neutron source removed. Three ionization chambers and three neutron counters were used in the safety and control system. They were placed in steel tubes with diameter about 7 cm and wall thickness about 1.5 mm, and were mounted at a distance of about 20 cm from the surface of the sphere. In Figure 2 the elements of the control and safety system are not shown. There was no other equipment in the room at the time of the experiments that might affect criticality.

The spherical tanks of outer diameters 66 cm, 88 cm, and 120 cm were made of stainless steel with thicknesses of 0.15 ± 0.02 cm, 0.19 ± 0.02 cm, and 0.21 ± 0.02 cm, respectively. The "effective" thickness of each spherical shell was determined, in addition, by weighing the empty tank and subsequently subtracting from the total weight the weights of individual elements, estimated by calculation (the neck, the flange, and others). The uncertainties of thicknesses were estimated as the maximum between the specified tolerance of the nominal value and the difference between the nominal value and the value determined by weighing.

The volume of each spherical tank was measured by water calibration prior to use. The exact value of the internal radius of each sphere was determined from the measured volume, assuming that the shape of the tank was exactly spherical. This assumption was confirmed by the fact that differences between the prescribed volumes of the spheres (150, 348, and 900 liters) and measured ones were even smaller than estimated uncertainties in measured volumes (see Table 1). Measurements were done[a] to confirm the spherical shape of the tanks, although the details of the measurements are not known.

Filling and pumping out of the solution were carried out through the neck. Feed of the solution into the sphere was metered in portions ranging from several milliliters up to 10 liters. The uncertainty of the volume of each portion varied from approximately $\pm$ 1 milliliter for portions with volumes smaller than 100 milliliters to $\pm$ 10 milliliters for portions with volumes of several liters. Filling of the core with solution was carried out through the polyethylene feed pipe. Solution was pumped out through another polyethylene tube (also used as a sampling tube) by means of a vacuum created in the pumping system.

For determination of the sphere volume, the needed number of 10-liter portions of water was flooded into the tank and then superfluous water was pumped out and its volume was measured. At that time, the level indicator position of the levelmeter was at the full-sphere position.

[a] Private communication, V. N. Gurin, January, 1997.

All nine assemblies were slightly supercritical. Excess reactivity was determined by positive period measurements. The dimensions and reactivity excesses are listed in Table 1.

Table 1. Critical Dimensions.

Case Number	Sphere Radius[a], cm	Volume, liters	Reactivity Excess, β_{eff}
1	32.95	126.3 ± 0.3	0.09
2	32.95	144.1 ± 0.3	0.04
3	32.95 (± 0.02)	149.9 ± 0.2	0.06
4	43.63	197.6 ± 0.5	0.06
5	43.63	318.6 ± 0.6	0.09
6	43.63 (± 0.02)	347.9 ± 0.4	0.12
7	59.89	501.8 ± 0.9	0.05
8	59.89	845.2 ± 1.4	0.04
9	59.89 (± 0.02)	899.8 ± 0.9	0.09

(a) Derived from full-sphere volume measurement.

In the experiments with truncated spheres, solutions of definite uranium concentrations were used and the approximately critical volumes were determined. In these cases a greater number of smaller portions of the solution was flooded into the tank. Consequently, the uncertainty of the volume determination was somewhat greater than the uncertainty of the determination of the total sphere volume. In the experiments with fully filled spheres, the volume of the solution was determined by the adjusted level indicator, and uranium concentrations in the solution were then determined by sampling. In these cases after each change of solution concentration the solution in the tank was carefully mixed by air sparging via a stainless steel tube (1.0 cm in diameter, 0.04 cm wall thickness). The concentration was determined as the average of three samples obtained from the bottom, from the middle, and from the upper part of the spherical tank.

All experiments were performed at room temperature (approximately 20°C).

1.3 Description of Material Data

The enrichment of uranium by ^{235}U according to certificate data was 10.0 wt.% (10.12 at.%) with no shown uncertainty. Therefore, the adopted uncertainty of this value was ± 0.05 wt.%. According to results of mass spectrometric analysis, the ^{235}U content is 10.26 ± 0.07 at.%. An average value was adopted (see Table 2). The ^{234}U at.% was estimated from the mass spectrometric analysis.

Table 2. Uranium Isotopic Composition.

Isotope	at.%
^{234}U	0.09 ± 0.04
^{235}U	10.19 ± 0.10
^{238}U	89.72 ± 0.10
Total:	100.00

The uranium solution was uranyl nitrate, $UO_2(NO_3)_2$ dissolved in nitric acid (HNO_3) and diluted with distilled water. The solution density was measured by hydrometer, with the value of one scale division equal to 0.001 g/cm^3. This value was adopted as the measure of the inaccuracy of the density determination.

The uranium concentration in the solution was measured by appropriate chemical methods. Two or three analyses were done for each solution. The range of the results always was smaller than method inaccuracies. So the latter (± 0.5%) was adopted as the measure of the uncertainty of the uranium concentration determination.

The concentration of free nitric acid in the solution was determined by the alkalimetric titration method. The uncertainty of this method is ± 1%.

Measured parameters of the solutions (uranium concentration, solution density, excess nitric acid concentration) are given in Table 3. These were the measured parameters for the supercritical configurations (see Table 1).

Table 3. Measured Solution Parameters.

Case Number	Uranium Concentration, grams/liter	Solution Density, grams/cm^3	Concentration of HNO_3, moles/liter
1	296.0 ± 1.5	1.444 ± 0.001	1.36 ± 0.01
2	264.0 ± 1.3	1.396 ± 0.001	1.19 ± 0.01
3	260.0 ± 1.3	1.391 ± 0.001	1.11 ± 0.01
4	255.0 ± 1.3	1.383 ± 0.001	1.14 ± 0.01
5	203.0 ± 1.0	1.305 ± 0.001	0.91 ± 0.01
6	197.0 ± 1.0	1.297 ± 0.001	0.89 ± 0.01
7	193.0 ± 1.0	1.291 ± 0.001	0.88 ± 0.01
8	171.0 ± 0.8	1.260 ± 0.001	0.83 ± 0.01
9	168.0 ± 0.8	1.256 ± 0.001	0.84 ± 0.01

All impurities in the solution were caused by the impurity of the uranyl nitrate used (not by water impurities). Concentrations of impurities in uranium dioxide determined by chemical analysis are given in Table 4. Uranium content in the uranium dioxide was 87.83 wt.%, according to the certificate on the uranium dioxide.

Table 4. Concentrations of Impurities in Uranium Dioxide.

Element	Wt.%
Fe	0.0470
C	< 0.0200
Ni	0.0054
Si	0.0040
N	0.0010
Mn	0.0018
Cu	0.0007
Co	< 0.0001
B	0.000018
Total:	0.080018

All spherical tanks and the auxiliary parts of the critical assemblies used in these experiments were made of 1X18H10T stainless steel. The stainless steel density was 7.93 g/cm^3. Its composition, according to the USSR State Standard 5632-72, is given in Table 5. Cited uncertainties are caused by possible deviations of the real composition from the normative one.

Table 5. Stainless Steel Composition.

Element	Wt.%
Fe	69.1 ± 0.7
Cr	18.0 ± 0.5
Ni	10.0 ± 0.5
Mn	1.5 ± 0.2
Si	0.8 ± 0.1
Ti	0.6 ± 0.1
Total	100.0

Concrete density and composition were not measured. A density of 2.3 g/cm^3 and a typical[a] composition listed in Table 6 were adopted for estimation of reflection of neutrons from the room's concrete walls and ceiling.

Table 6. Concrete Composition.

Element	Wt.%
O	49.0
Ca	23.0
Si	16.0
C	6.0
Al	2.0
Fe	1.0
Mg	1.0
P	1.0
H	1.0
Total:	100.0

1.4 Supplemental Experimental Measurements

No additional experimental data were found.

[a] Бродер Д. Л. и др. Бетон в защите ядерных установок. Москва, Атомиздат, 1973. (Broder D. L. et al., "Concrete in Shielding of Nuclear Facilities." Moscow. Atomizdat, 1973, in Russian.)

2.0 EVALUATION OF EXPERIMENTAL DATA

Inaccuracy of the determination of criticality caused by uncertainties of the following parameters was estimated:

- in isotopic composition of uranium;
- in uranium concentration in solution;
- in solution density;
- in HNO_3 concentration in solution;
- in critical volume.

As estimated by direct calculations, concentrations of impurities in the solution (see Table 4) were so small that their influence on k_{eff} in all nine cases was less than 0.01%. Thus it was not necessary to estimate the influence of uncertainties of these concentrations on the k_{eff} uncertainty.

Sensitivity of k_{eff} to the uncertainty of the i-th solution constituent atomic density,

$$I_i = \frac{\Delta k}{\Delta N_i} \cdot \frac{N_i}{k}$$

was calculated by perturbation theory using spherical critical models of assemblies. Calculations were performed with a P_1-approximation by means of the CRAB-1 code and the ABBN-90[a] group constant set ("90" refers to the year 1990).

Assuming that the isotopic content of ^{235}U is strongly correlated with the content of ^{238}U and only slightly correlated with the content of ^{234}U, the inaccuracy of k_{eff} caused by the uncertainty in isotope composition was calculated by the formula:

$$\delta k_{\varepsilon} = \sqrt{\left(\frac{\Delta N_{235}}{N_{235}} \cdot I_{235} - \frac{\Delta N_{238}}{N_{238}} \cdot I_{238}\right)^2 + \left(\frac{\Delta N_{234}}{N_{234}} \cdot I_{234}\right)^2}$$

Here N_{235}, N_{238}, N_{234}, and ΔN_{235}, ΔN_{238}, ΔN_{234} are uranium isotope atom percents and their standard deviations from Table 2.

The inaccuracies of k_{eff} caused by the uncertainties of the uranium and HNO_3 concentrations in solution were calculated by the formulas given below. In the formulas, $\Delta N_H(\Delta\rho_i)$ and $\Delta N_O(\Delta\rho_i)$ are variations of hydrogen and oxygen atomic densities caused by variation of the i-th constituent density. Formulas given in Section 3.3 are used for the calculation of N_H and N_O. Variations ΔN_H and ΔN_O were calculated by numerical differentiation and by assuming changes in the i-th constituent density of one standard deviation.

[a] RSIC DLC-182 "ABBN-90: Multigroup Constant Set for Calculation of Neutron and Photon Radiation Fields and Functionals, Including the CONSYST2 Program."

$$\delta k_U = \frac{\Delta\rho_U}{\rho_U}\cdot(I_{235} + I_{238} + I_{234}) + \frac{\Delta N_H(\Delta\rho_U)}{N_H}\cdot I_H + \frac{\Delta N_O(\Delta\rho_U)}{N_O}\cdot I_O$$

Here ρ_U and $\Delta\rho_U$ are the uranium density and its standard deviation from Table 3.

$$\delta k_{HNO3} = \frac{\Delta N^a}{N^a}\cdot I_N + \frac{\Delta N_H(\Delta N^a)}{N_H}\cdot I_H + \frac{\Delta N_O(\Delta N^a)}{N_O}\cdot I_O$$

Here N^a and ΔN^a are the HNO_3 concentration and its standard deviation from Table 3.

The inaccuracy of k_{eff} caused by the uncertainty of solution density was calculated by the formula:

$$\delta k_{sol} = \frac{\Delta N_H(\Delta\rho_{sol})}{N_H}\cdot I_H + \frac{\Delta N_O(\Delta\rho_{sol})}{N_O}\cdot I_O$$

Here $\Delta\rho_{sol}$ is the standard deviation of solution density from Table 3.

Inaccuracies caused by uncertainties of critical volume, δk_V, also were estimated using spherical models of assemblies. Sensitivities were calculated by the direct variation of core radius. Data given in Table 1 were used.

In Table 7 the constituents of the inaccuracy of k_{eff} are listed for all assemblies of the considered series. In the last column, the summary inaccuracy of k_{eff} is given:

$$\delta k = \sqrt{\delta k_\varepsilon^{\,2} + \delta k_U^{\,2} + \delta k_{sol}^{\,2} + \delta k_{HNO3}^{\,2} + \delta k_V^{\,2}}$$

Table 7. Constituents of the Inaccuracy of k_{eff} (percents).

Case Number	δk_ε	δk_U	δk_{HNO3}	δk_{sol}	δk_V	δk
1	0.37	0.11	0.06	0.02	0.03	0.39
2	0.39	0.14	0.05	0.01	0.03	0.42
3	0.39	0.14	0.05	0.01	0.02	0.42
4	0.39	0.15	0.05	0.01	0.03	0.42
5	0.43	0.20	0.04	0.01	0.01	0.48
6	0.44	0.21	0.04	0.01	0.01	0.49
7	0.44	0.21	0.04	0.01	0.01	0.49
8	0.46	0.23	0.04	0.02	0.01	0.52
9	0.46	0.24	0.04	0.02	0.01	0.52

3.0 BENCHMARK SPECIFICATION

3.1 Description of Model

3.1.1 Description of Simplifications - Benchmark models were designed on the basis of realistic calculational models of the critical experiments by using a series of simplifications. Three types of experimental details were neglected after evaluating their influence on criticality:

- impurity in fissile solution;
- small constructive details in and around the assembly;
- reflection of neutrons from the room walls, floor, and ceiling.

3.1.2 Influence of the Elimination of Impurities - As was pointed out in Section 2, the influence of solution impurities on k_{eff} was negligibly small. Thus impurities are not included in the benchmark models, and no correction of k_{eff} was made.

3.1.3 Influence of the Elimination of Structure Details and Surroundings - The spherical models of Cases 3, 6, and 9 were constructed for estimation of the neck, upper plate, empty cylindrical tank, details of the control system, and wall, floor, and ceiling influence on k_{eff}. Calculations were performed with a P_1-approximation by means of the CRAB-1 code and the ABBN-90 group constant set. Eight spherical shells surrounding the core with thicknesses ranging from 1 cm to 100 cm were used for modeling the mentioned details. Materials of all details were distributed uniformly over the volume of the corresponding shell. It was found that the summary effect of all details on k_{eff} was equal to 0.1%. The uncertainty of this value is estimated as 50%. This bias is included in the benchmark-model k_{eff}'s given in Section 3.5.

The filling tube, pumping out tube, and sparger tube were in the sphere when the reactivities of the benchmark configurations were measured. The effect of these tubes was found to be negligible by means of the CRAB-1 code using perturbation theory. Therefore, they are not included in the model.

3.2 Dimensions

The basic model was a bare spherical stainless steel shell containing uranyl nitrate solution.

The dimensions of the benchmark calculational models are given in Table 8. Inner radii of the spherical shells were derived from the reported full-sphere volumes (see Table 1). Models of Cases 3, 6, and 9 are spherical systems. The other models are truncated spheres of solutions in the spherical steel shells. The solution surface is always above the center of the sphere. The solution height in Table 8 is the distance between the solution surface and the center of the sphere (radius for the full spheres).

Table 8. Geometrical Sizes of Benchmark Models.

Case Number	Spherical Shell Inner Radius,[a] cm	Spherical Shell Thickness, cm	Solution Height,[a] cm
1	32.9537	0.15	16.4073
2	32.9537	0.15	25.1548
3	32.9537	0.15	32.9537
4	43.6303	0.19	3.9656
5	43.6303	0.19	28.0537
6	43.6303	0.19	43.6303
7	59.8897	0.21	4.6151
8	59.8897	0.21	41.9340
9	59.8897	0.21	59.8897

(a) Derived values are given to higher precision than the data to prevent propagation of error from unnecessary roundoff.

3.3 Material Data

3.3.1 Core Nuclear Densities - The nuclear densities of the individual uranium isotopes are given by:

$$N_i = \frac{\rho_U \, N_A \, A_{f,i}}{A_{w,U}}, \text{ for } i = {}^{234}U, {}^{235}U, {}^{238}U.$$

Here: N_i is an atomic density of isotope "i";
$A_{f,i}$ is the atom fraction of isotope "i" (see at.%'s in Table 2);
ρ_U is the total density of uranium in solution in g/cm^3 (see Table 3);
$A_{w,U}$ is the atomic weight of uranium
($A_{w,U} = A_{w,234} \times A_{f,234} + A_{w,235} \times A_{f,235} + A_{w,238} \times A_{f,238}$);
N_A is Avogadro's number.

The mass density of uranyl nitrate, $UO_2(NO_3)_2$, is given by:

$$\rho_{UO2(NO3)2} = \frac{N_U \, M_{w,UO2(NO3)2}}{N_A}$$

where: $N_U = N_{234} + N_{235} + N_{238}$ is the total uranium atomic density;
$M_{w,UO2(NO3)2}$ is the molecular weight of uranyl nitrate.

The mass density of nitric acid, HNO_3, in g/cm^3 is given by:

$$\rho_{HNO3} = N^a \, M_{w,HNO3}$$

where: N^a is the total density of HNO_3 in moles/cm^3 (see Table 3);
$M_{w,\ HNO3}$ is the molecular weight of nitric acid.

The mass density of water in the solution can then be determined by difference:

$$\rho_{H2O} = \rho_{sol} - \rho_{UO2(NO3)2} - \rho_{HNO3}$$

Here ρ_{sol} is given in Table 3.

The total atom densities of nitrogen, N_N, oxygen, N_O, and hydrogen, N_H are then determined by the following formulas:

$$N_N = 2 \cdot N_U + N_A \cdot N^a$$

$$N_O = 8 \cdot N_U + N_A \cdot \left(\frac{\rho_{H2O}}{M_{w,\ H2O}} + 3 \cdot \frac{\rho_{HNO3}}{M_{w,\ HNO3}} \right)$$

$$N_H = N_A \cdot \left(2 \cdot \frac{\rho_{H2O}}{M_{w,\ H2O}} + \frac{\rho_{HNO3}}{M_{w,\ HNO3}} \right)$$

Here $M_{w,\ H2O}$ is the molecular weight of water, and ρ_{H2O} and ρ_{HNO3} in g/cm^3 are calculated by the above formulas.

Using the above equations, solution atom densities were calculated. Results of these calculations are given in Table 9.

Table 9. Calculated Solution Atom Densities (atoms/barn-cm).

Case Number	N_{234}	N_{235}	N_{238}	N_N	N_O	N_H
1	6.7481×10^{-7}	7.6403×10^{-5}	6.7271×10^{-4}	2.3185×10^{-3}	3.7473×10^{-2}	5.8854×10^{-2}
2	6.0186×10^{-7}	6.8143×10^{-5}	5.9998×10^{-4}	2.0540×10^{-3}	3.7042×10^{-2}	5.9802×10^{-2}
3	5.9274×10^{-7}	6.7111×10^{-5}	5.9089×10^{-4}	1.9856×10^{-3}	3.7040×10^{-2}	6.0199×10^{-2}
4	5.8134×10^{-7}	6.5820×10^{-5}	5.7953×10^{-4}	1.9783×10^{-3}	3.6939×10^{-2}	6.0110×10^{-2}
5	4.6279×10^{-7}	5.2398×10^{-5}	4.6135×10^{-4}	1.5764×10^{-3}	3.6225×10^{-2}	6.1483×10^{-2}
6	4.4911×10^{-7}	5.0849×10^{-5}	4.4771×10^{-4}	1.5340×10^{-3}	3.6175×10^{-2}	6.1685×10^{-2}
7	4.3999×10^{-7}	4.9817×10^{-5}	4.3862×10^{-4}	1.5077×10^{-3}	3.6117×10^{-2}	6.1763×10^{-2}
8	3.8984×10^{-7}	4.4138×10^{-5}	3.8862×10^{-4}	1.3661×10^{-3}	3.5868×10^{-2}	6.2307×10^{-2}
9	3.8300×10^{-7}	4.3364×10^{-5}	3.8181×10^{-4}	1.3569×10^{-3}	3.5837×10^{-2}	6.2336×10^{-2}

3.3.2 Atom Densities of the Structure - Atom densities of stainless steel constituents were calculated from weight percents given in Table 5 and density of 7.93 g/cm^3. Data are given in Table 10.

Table 10. Atom Densities for Stainless Steel Spherical Shells.

Element	Atom Density, atoms/(barn $\times$ cm)
Fe	5.9088×10^{-2}
Cr	1.6532×10^{-2}
Ni	8.1369×10^{-3}
Mn	1.3039×10^{-3}
Si	1.3603×10^{-3}
Ti	5.9844×10^{-4}

3.4 Temperature Data

All experiments were performed at room temperature (approximately 20°C). The temperature of 300 K was assumed for calculations.

3.5 Experimental and Benchmark-Model k_{eff}

The CRAB-1 code and the ABBN-90 group constant set were used for estimating β_{eff}. Spherical critical models of the assemblies were used in the calculations. The following values were obtained.

Table 11. Calculated Reactivities and β_{eff}'s of the Considered Assemblies.

Case Number	Reactivity Excess, β_{eff}	β_{eff}	k_{eff}
1	0.09	0.0078	1.0007
2	0.04	0.0077	1.0003
3	0.06	0.0077	1.0005
4	0.06	0.0077	1.0005
5	0.09	0.0074	1.0007
6	0.12	0.0074	1.0009
7	0.05	0.0074	1.0004
8	0.04	0.0072	1.0003
9	0.09	0.0072	1.0006

The uncertainty in β_{eff} is estimated as 8%. This uncertainty leads to a 0.01%-uncertainty in k_{eff}.

Reducing the rigorous experimental models to simplified benchmark models leads to biasing of k_{eff}, as described in Section 3.1. Uncertainties of experimental data result in an uncertainty of k_{eff}, as described in Section 2. Experimental and benchmark-model k_{eff}'s are shown in Table 12. Bias and β_{eff} uncertainties are also included in the benchmark-model k_{eff} uncertainty.

Table 12. Experimental and Benchmark-Model k_{eff}'s.

Case Number	H to ^{235}U Atom Ratio	Experimental k_{eff}[(a)]	Benchmark-Model k_{eff}
1	770	1.0007 ± 0.0039	0.9997 ± 0.0039
2	878	1.0003 ± 0.0042	0.9993 ± 0.0042
3	897	1.0005 ± 0.0042	0.9995 ± 0.0042
4	913	1.0005 ± 0.0042	0.9995 ± 0.0042
5	1173	1.0007 ± 0.0048	0.9997 ± 0.0048
6	1213	1.0009 ± 0.0049	0.9999 ± 0.0049
7	1240	1.0004 ± 0.0049	0.9994 ± 0.0049
8	1412	1.0003 ± 0.0052	0.9993 ± 0.0052
9	1438	1.0006 ± 0.0052	0.9996 ± 0.0052

(a) Experimental k_{eff} uncertainties include those uncertainties identified in Section 2.0.

4.0 RESULTS OF SAMPLE CALCULATIONS

Sample calculational results are shown in Tables 13.a and 13.b. Details of the calculations including code input listings are provided in Appendix A. Some calculations were performed using nonstandard code/cross section set combinations. The results of these calculations are given in Appendix B.

Some of the KENO Hansen-Roach values are more than 1% high. However, since Hansen-Roach cross sections were developed for fast highly-enriched metal systems, they are not expected to give correct results for thermal low-enriched solution systems.

Table 13.a. Sample Calculation Results (Russian Federation).

Code (Cross Section Set) → Configuration ↓	MCU (DLC-MCU)	MMK (ABBN-90)
1	0.9958 ± 0.0008	1.0048 ± 0.0013
2	0.9941 ± 0.0008	1.0013 ± 0.0012
3	0.9986 ± 0.0008	1.0070 ± 0.0011
4	0.9912 ± 0.0008	1.0016 ± 0.0013
5	0.9956 ± 0.0007	1.0032 ± 0.0010
6	0.9955 ± 0.0007	1.0046 ± 0.0010
7	0.9957 ± 0.0007	1.0036 ± 0.0009
8	0.9982 ± 0.0006	1.0079 ± 0.0008
9	0.9972 ± 0.0006	1.0043 ± 0.0008

Table 13.b. Sample Calculation Results (United States).[(a)]

Code (Cross Section Set) → Configuration ↓	KENO (Hansen-Roach)	KENO (27-Group ENDF/B-IV)	MCNP (Continuous Energy ENDF/B-V)	ONEDANT (27-Group ENDF/B-IV)
1	1.0069 ± 0.0007	0.9986 ± 0.0006	0.9994 ± 0.0004	--
2	1.0064 ± 0.0007	0.9962 ± 0.0006	0.9981 ± 0.0004	--
3	1.0110 ± 0.0006	1.0010 ± 0.0006	1.0016 ± 0.0004	1.0022
4	1.0049 ± 0.0007	0.9945 ± 0.0006	0.9943 ± 0.0004	--
5	1.0132 ± 0.0006	0.9962 ± 0.0005	0.9983 ± 0.0003	--
6	1.0144 ± 0.0005	0.9972 ± 0.0005	0.9987 ± 0.0003	0.9987
7	1.0129 ± 0.0005	0.9940 ± 0.0005	0.9969 ± 0.0003	--
8	1.0177 ± 0.0005	0.9970 ± 0.0004	1.0000 ± 0.0003	--
9	1.0155 ± 0.0004	0.9940 ± 0.0004	0.9979 ± 0.0003	0.9940

(a) Results supplied by authors.

5.0 REFERENCES

1. A. V. Kamaev, V. N. Gurin, G. M. Vladykov et al., "The Analysis of the Critical Parameters of Homogeneous Spherical Assemblies," in: "The Physics of Nuclear Reactors", collected articles, vol. 3, pp. 63-84 (Obninsk, 1966).

2. B. G. Dubovskii, A. V. Kamaev, G. M. Vladykov et al., "The Critical Parameters of Aqueous Solutions of $UO_2(NO_3)_2$ and the Interaction of Subcritical Homogeneous Assemblies," in Proceedings of the Symposium Criticality Control of Fissile Materials, Stockholm, 1-5 November 1965 (International Atomic Energy Agency, Vienna, 1966), pp.267-278.

APPENDIX A: TYPICAL INPUT LISTINGS

A.1 MCU Input Listings

The MCU-RFFI calculations were run with 5,000 generations of 200 histories per generation. No generations were skipped. So, the results were based on 1,000,000 active neutron histories.

MCU Input Listing for Case 1 of Table 13.a.

```
TEMPR* 300.
FZONE* 1,300.
U234:6.7481E-7
U235:7.6403E-5
U238:6.7271E-4
N:2.3185E-3
O:3.7473E-2
H:5.8854E-2
FZONE* 2,300.
FE:5.9088E-2
CR:1.6532E-2
NI:8.1369E-3
MN:1.3039E-3
SI:1.3603E-3
TI:5.9844E-4
FZONE* 3,300
N:3.5214E-5
O:1.5092E-5
FINISH
CONT  0 0 0
SPH N1  0 0 0 33.1037
BCON    B
SPH N2  0 0 0 32.9537
SLB N3  0 0 1 -32.9537 16.4073
END
ZON1     2 3       A1:1
ZON2     1 -2      A2:2
ZON3     2 -3      A3:3
END
FINISH
SPNT   0.  0.  0.
FINISH
FINISH
NAMVAR LST003-1
NTOT   200
NBAT   5
FINISH
NAMVAR LST003-1
MAXSER 1000
DTZML  10.
NPRI   200
FULL
FINISH
```

MCU Input Listing for Case 2 of Table 13.a.

```
TEMPR* 300.
FZONE* 1,300.
U234:6.0186E-7
U235:6.8143E-5
U238:5.9998E-4
N:2.0540E-3
O:3.7042E-2
H:5.9802E-2
FZONE* 2,300.
FE:5.9088E-2
CR:1.6532E-2
NI:8.1369E-3
MN:1.3039E-3
SI:1.3603E-3
TI:5.9844E-4
FZONE* 3,300
N:3.5214E-5
O:1.5092E-5
FINISH
CONT  0 0 0
SPH N1  0 0 0 33.1037
BCON    B
SPH N2  0 0 0 32.9537
SLB N3  0 0 1 -32.9537 25.1548
END
ZON1     2 3       A1:1
ZON2     1 -2      A2:2
ZON3     2 -3      A3:3
END
FINISH
SPNT   0.  0.  0.
FINISH
FINISH
NAMVAR LST003-2
NTOT   200
NBAT   5
FINISH
NAMVAR LST003-2
MAXSER 1000
DTZML  10.
NPRI   200
FULL
FINISH
```

MCU Input Listing for Case 3 of Table 13.a.

```
TEMPR* 300.
FZONE* 1,300.
U234:5.9274E-7
U235:6.7111E-5
U238:5.9089E-4
N:1.9856E-3
O:3.7040E-2
H:6.0199E-2
FZONE* 2,300.
FE:5.9088E-2
CR:1.6532E-2
NI:8.1369E-3
MN:1.3039E-3
SI:1.3603E-3
TI:5.9844E-4
FINISH
CONT  0 0 0
SPH N1  0 0 0 33.1037
BCON    B
SPH N2  0 0 0 32.9537
END
ZON1     2         A1:1
ZON2     1 -2      A2:2
END
FINISH
SPNT   0.  0.  0.
FINISH
FINISH
NAMVAR LST003-3
NTOT   200
NBAT   5
FINISH
NAMVAR LST003-3
MAXSER 1000
DTZML  10.
NPRI   200
FULL
FINISH
```

MCU Input Listing for Case 4 of Table 13.a.

```
TEMPR* 300.
FZONE* 1,300.
U234:5.8134E-7
U235:6.5820E-5
U238:5.7953E-4
N:1.9783E-3
O:3.6939E-2
H:6.0110E-2
FZONE* 2,300.
FE:5.9088E-2
CR:1.6532E-2
NI:8.1369E-3
MN:1.3039E-3
SI:1.3603E-3
TI:5.9844E-4
FZONE* 3,300
N:3.5214E-5
O:1.5092E-5
FINISH
CONT  0 0 0
SPH N1  0 0 0 43.8203
BCON    B
SPH N2  0 0 0 43.6303
SLB N3  0 0 1 -43.6303 3.9656
END
ZON1     2 3       A1:1
ZON2     1 -2      A2:2
ZON3     2 -3      A3:3
END
FINISH
SPNT   0.  0.  0.
FINISH
FINISH
NAMVAR LST003-4
NTOT   200
NBAT   5
FINISH
NAMVAR LST003-4
MAXSER 1000
DTZML  10.
NPRI   200
FULL
FINISH
```

MCU Input Listing for Case 5 of Table 13.a.

```
TEMPR* 300.
FZONE* 1,300.
U234:4.6279E-7
U235:5.2398E-5
U238:4.6135E-4
N:1.5764E-3
O:3.6225E-2
H:6.1483E-2
FZONE* 2,300.
FE:5.9088E-2
CR:1.6532E-2
NI:8.1369E-3
MN:1.3039E-3
SI:1.3603E-3
TI:5.9844E-4
FZONE* 3,300
N:3.5214E-5
O:1.5092E-5
FINISH
CONT  0 0 0
SPH N1  0 0 0 43.8203
BCON    B
SPH N2  0 0 0 43.6303
SLB N3  0 0 1 -43.6303 28.0537
END
ZON1     2 3       A1:1
ZON2     1 -2      A2:2
ZON3     2 -3      A3:3
END
FINISH
SPNT   0.  0.  0.
FINISH
FINISH
NAMVAR LST003-5
NTOT   200
NBAT   5
FINISH
NAMVAR LST003-5
MAXSER 1000
DTZML  10.
NPRI   200
FULL
FINISH
```

MCU Input Listing for Case 6 of Table 13.a.

```
TEMPR* 300.
FZONE* 1,300.
U234:4.4911E-7
U235:5.0849E-5
U238:4.4771E-4
N:1.5340E-3
O:3.6175E-2
H:6.1685E-2
FZONE* 2,300.
FE:5.9088E-2
CR:1.6532E-2
NI:8.1369E-3
MN:1.3039E-3
SI:1.3603E-3
TI:5.9844E-4
FINISH
CONT  0 0 0
SPH N1  0 0 0 43.8203
BCON    B
SPH N2  0 0 0 43.6303
END
ZON1     2         A1:1
ZON2     1 -2      A2:2
END
FINISH
SPNT   0.  0.  0.
FINISH
FINISH
NAMVAR LST003-6
NTOT   200
NBAT   5
FINISH
NAMVAR LST003-6
MAXSER 1000
DTZML  10.
NPRI   200
FULL
FINISH
```

MCU Input Listing for Case 7 of Table 13.a.

```
TEMPR* 300.
FZONE* 1,300.
U234:4.3999E-7
U235:4.9817E-5
U238:4.3862E-4
N:1.5077E-3
O:3.6117E-2
H:6.1763E-2
FZONE* 2,300.
FE:5.9088E-2
CR:1.6532E-2
NI:8.1369E-3
MN:1.3039E-3
SI:1.3603E-3
TI:5.9844E-4
FZONE* 3,300
N:3.5214E-5
O:1.5092E-5
FINISH
CONT  0 0 0
SPH N1  0 0 0 60.0997
BCON    B
SPH N2  0 0 0 59.8897
SLB N3  0 0 1 -59.8897 4.6151
END
ZON1     2 3       A1:1
ZON2     1 -2      A2:2
ZON3     2 -3      A3:3
END
FINISH
SPNT   0.  0.  0.
FINISH
FINISH
NAMVAR LST003-7
NTOT   200
NBAT   5
FINISH
NAMVAR LST003-7
MAXSER 1000
DTZML  10.
NPRI   200
FULL
FINISH
```

MCU Input Listing for Case 8 of Table 13.a.

```
TEMPR* 300.
FZONE* 1,300.
U234:3.8984E-7
U235:4.4138E-5
U238:3.8862E-4
N:1.3661E-3
O:3.5868E-2
H:6.2307E-2
FZONE* 2,300.
FE:5.9088E-2
CR:1.6532E-2
NI:8.1369E-3
MN:1.3039E-3
SI:1.3603E-3
TI:5.9844E-4
FZONE* 3,300
N:3.5214E-5
O:1.5092E-5
FINISH
CONT  0 0 0
SPH N1  0 0 0 60.0997
BCON    B
SPH N2  0 0 0 59.8897
SLB N3  0 0 1 -59.8897 41.9340
END
ZON1     2 3       A1:1
ZON2     1 -2      A2:2
ZON3     2 -3      A3:3
END
FINISH
SPNT   0.  0.  0.
FINISH
FINISH
NAMVAR LST003-8
NTOT   200
NBAT   5
FINISH
NAMVAR LST003-8
MAXSER 1000
DTZML  10.
NPRI   200
FULL
FINISH
```

MCU Input Listing for Case 9 of Table 13.a.

```
TEMPR* 300.
FZONE* 1,300.
U234:3.8300E-7
U235:4.3364E-5
U238:3.8181E-4
N:1.3569E-3
O:3.5837E-2
H:6.2336E-2
FZONE* 2,300.
FE:5.9088E-2
CR:1.6532E-2
NI:8.1369E-3
MN:1.3039E-3
SI:1.3603E-3
TI:5.9844E-4
FINISH
CONT  0 0 0
SPH N1  0 0 0 60.0997
BCON    B
SPH N2  0 0 0 59.8897
END
ZON1     2         A1:1
ZON2     1 -2      A2:2
END
FINISH
SPNT   0.  0.  0.
FINISH
FINISH
NAMVAR LST003-9
NTOT   200
NBAT   5
FINISH
NAMVAR LST003-9
MAXSER 1000
DTZML  10.
NPRI   200
FULL
FINISH
```

A.2 MMK Input Listings

The MMKFK-2 code with the 26-group ABBN-90 cross section set was used for the calculations.

Resonance shielding was taken into account using the Bondarenko factors. Neutron current averaging of transport cross sections was used. Elastic slowing down was taken into account, not by group slowing down cross sections but by modeling of the slowing down process using constant self-shielded scattering and absorption cross sections within each group.

Two hundred neutrons per generation were used in the calculations. The first 5 generations were used only for the establishment of the source distribution and were excluded from the statistics. The results were based on 250,000 active neutron histories.

MMK Input Listing for Case 1 of Table 13.a.

```
0  0
26  12  3  0  0
0  0  0  0
U234      U235      U238      N         O
FE        CR        NI        MN        SI
TI        H
300. 300. 300.
.000000675.000076403.00067271 .0023185  .037473
0.        0.        0.        0.        0.
0.        .058854
0.        0.        0.        0.        0.
.059088   .016532   .0081369  .0013039  .0013603
.00059844 0.
0.        0.        0.        0.        .000000001
0.        0.        0.        0.        0.
0.        0.
2  0
Y
DATM
DATMMK    JEVG1     26        3
59        0         -1
0         1         250000    200       5
SHSHH
2  0
0.  0.  0.  33.1037  0
2
0.  0.  0.  32.9537  1
49.36
1  3
0. 1. 0.
ENDG
```

MMK Input Listing for Case 2 of Table 13.a.

```
0  0
26  12  3  0  0
0  0  0  0
U234      U235      U238      N         O
FE        CR        NI        MN        SI
TI        H
300. 300. 300.
.000000602.000068143.00059998 .0020540  .037042
0.        0.        0.        0.        0.
0.        .059802
0.        0.        0.        0.        0.
.059088   .016532   .0081369  .0013039  .0013603
.00059844 0.
0.        0.        0.        0.        .000000001
0.        0.        0.        0.        0.
0.        0.
2  0
Y
DATM
DATMMK    JEVG2     26        3
59        0         -1
0         1         250000    200       5
SHSHH
2  0
0.  0.  0.  33.1037  0
2
0.  0.  0.  32.9537  1
58.1085
1  3
0. 1. 0.
ENDG
```

MMK Input Listing for Case 3 of Table 13.a.

```
0  0
26  12  3  0  0
0  0  0  0
U234      U235      U238      N         O
FE        CR        NI        MN        SI
TI        H
300. 300. 300.
.000000593.000067111.00059089 .0019856  .037042
0.        0.        0.        0.        0.
0.        .060199
0.        0.        0.        0.        0.
.059088   .016532   .0081369  .0013039  .0013603
.00059844 0.
0.        0.        0.        0.        .000000001
0.        0.        0.        0.        0.
0.        0.
2  0
Y
DATM
DATMMK    JEVG3     26        3
59        0         -1
0         1         250000    200       5
SHSHH
2  0
0.  0.  0.  33.1037  0
2
0.  0.  0.  32.9537  0
1
0. 1.
ENDG
```

MMK Input Listing for Case 4 of Table 13.a.

```
0  0
26  12  3  0  0
0  0  0  0
U234      U235      U238      N         O
FE        CR        NI        MN        SI
TI        H
300. 300. 300.
.000000581.00006582 .00057953 .0019783  .036939
0.        0.        0.        0.        0.
0.        .060110
0.        0.        0.        0.        0.
.059088   .016532   .0081369  .0013039  .0013603
.00059844 0.
0.        0.        0.        0.        .000000001
0.        0.        0.        0.        0.
0.        0.
2  0
Y
DATM
DATMMK    JEVG4     26        3
59        0         -1
0         1         250000    200       5
SHSHH
2  0
0.  0.  0.  43.8203  0
2
0.  0.  0.  43.6303  1
47.5959
1  3
0. 1. 0.
ENDG
```

MMK Input Listing for Case 5 of Table 13.a.

```
0  0
26  12  3  0  0
0  0  0  0
U234      U235      U238      N         O
FE        CR        NI        MN        SI
TI        H
300. 300. 300.
.000000463.000052398.00046135 .0015764  .036225
0.        0.        0.        0.        0.
0.        .061483
0.        0.        0.        0.        0.
.059088   .016532   .0081369  .0013039  .0013603
.00059844 0.
0.        0.        0.        0.        .000000001
0.        0.        0.        0.        0.
0.        0.
2  0
Y
DATM
DATMMK    JEVG5     26        3
59        0         -1
0         1         250000    200       5
SHSHH
2  0
0.  0.  0.  43.8203  0
2
0.  0.  0.  43.6303  1
71.684
1  3
0. 1. 0.
ENDG
```

MMK Input Listing for Case 6 of Table 13.a.

```
0  0
26  12  3  0  0
0  0  0  0
U234      U235      U238      N         O
FE        CR        NI        MN        SI
TI        H
300. 300. 300.
.000000449.000050849.00044771 .0015340  .036175
0.        0.        0.        0.        0.
0.        .061685
0.        0.        0.        0.        0.
.059088   .016532   .0081369  .0013039  .0013603
.00059844 0.
0.        0.        0.        0.        .000000001
0.        0.        0.        0.        0.
0.        0.
2  0
Y
DATM
DATMMK    JEVG6     26        3
59        0         -1
0         1         250000    200       5
SHSHH
2  0
0.  0.  0.  43.8203  0
2
0.  0.  0.  43.6303  0
1
0. 1.
ENDG
```

MMK Input Listing for Case 7 of Table 13.a.

```
0  0
26  12  3  0  0
0  0  0  0
U234      U235      U238      N         O
FE        CR        NI        MN        SI
TI        H
300. 300. 300.
.000000440.000049817.00043862 .0015077  .036117
0.        0.        0.        0.        0.
0.        .061763
0.        0.        0.        0.        0.
.059088   .016532   .0081369  .0013039  .0013603
.00059844 0.
0.        0.        0.        0.        .000000001
0.        0.        0.        0.        0.
0.        0.
2  0
Y
DATM
DATMMK    JEVG7     26        3
59        0         -1
0         1         640000    200       5
SHSHH
2  0
0.  0.  0.  60.0997  0
2
0.  0.  0.  59.8897  1
64.5048
1  3
0. 1. 0.
ENDG
```

MMK Input Listing for Case 8 of Table 13.a.

```
0  0
26  12  3  0  0
0  0  0  0
U234      U235      U238      N         O
FE        CR        NI        MN        SI
TI        H
300. 300. 300.
.000000390.000044138.00038862 .0013661  .035868
0.        0.        0.        0.        0.
0.        .062307
0.        0.        0.        0.        0.
.059088   .016532   .0081369  .0013039  .0013603
.00059844 0.
0.        0.        0.        0.        .000000001
0.        0.        0.        0.        0.
0.        0.
2  0
Y
DATM
DATMMK    JEVG8     26        3
99        0         -1
0         1         640000    200       5
SHSHH
2  0
0.  0.  0.  60.0997  0
2
0.  0.  0.  59.8897  1
101.8237
1  3
0. 1. 0.
ENDG
```

MMK Input Listing for Case 9 of Table 13.a.

```
0  0
26  12  3  0  0
0  0  0  0
U234      U235      U238      N         O
FE        CR        NI        MN        SI
TI        H
300. 300. 300.
.000000383.000043364.00038181 .0013569  .035837
0.        0.        0.        0.        0.
0.        .062336
0.        0.        0.        0.        0.
.059088   .016532   .0081369  .0013039  .0013603
.00059844 0.
0.        0.        0.        0.        .000000001
0.        0.        0.        0.        0.
0.        0.
2  0
Y
DATM
DATMMK    JEVG9     26        3
99        0         -1
0         1         640000    200       5
SHSHH
2  0
0.  0.  0.  60.0997  0
2
0.  0.  0.  59.8897  0
1
0. 1.
ENDG
```

A.3 KENO Input Listings

Hansen-Roach Cross Sections

The inputs given below are for the 16-group Hansen-Roach "stand-alone" version of KENO-5A. The problems were run with 1,000,000 active and 25,000 inactive histories (400 active generations, ten skipped generations, and 2500 histories/generation). These problems were also run with the KENO-5A code with the ORNL SCALE4.3 code system using Hansen-Roach cross sections and the CSAS option. k_{eff} results are listed in Table A.1.

Table A.1. Sample Calculation Results (United States).[a]

Case Number	KENO (Hansen-Roach, CSAS)
1	1.0060 ± 0.0007
2	1.0065 ± 0.0006
3	1.0104 ± 0.0006
4	1.0032 ± 0.0006
5	1.0119 ± 0.0005
6	1.0115 ± 0.0005
7	1.0116 ± 0.0006
8	1.0171 ± 0.0005
9	1.0147 ± 0.0004

(a) Results supplied by authors.

For the "stand-alone" version of KENO-5A with Hansen-Roach cross sections, values of σ_p were computed for ^{235}U and ^{238}U using the Bondarenko formalism for scattering cross sections, 20.45, 3.89 and 9.96 barns for hydrogen, oxygen, and nitrogen, respectively. The computed σ_p values for ^{235}U are higher than those tabulated with the cross sections, so the infinite dilute cross sections were used. The round-off σ_p values for ^{238}U used for calculations are listed in Table A.2. Linear interpolation of cross section sets was used.

Table A.2. Hansen-Roach σ_p Values for ^{238}U.

Case Number	σ_p
1	2000
2	2300
3	2400
4	2400
5	3100
6	3200
7	3200
8	3700
9	3700

27-Group ENDF/B-IV Cross Sections

The 27-group inputs given below are for the KENO-5A code as run with the ORNL SCALE4.3 code system using the CSAS option. The problems were run with 1,000,000 active and 25,000 inactive histories (400 active generations, ten skipped generations, and 2500 histories/generation).

KENO-5A Input Listing for Case 1 of Table 13.b (16-Energy-Group Hansen-Roach Cross Sections).

```
LEU-SOL-THERM-003-1
READ PARAMETERS
LIB=41
TME=360
GEN=410
NPG=2500
NSK=10
END PARAMETERS
READ MIXT
MIX=1
92400 6.7481E-7
92500 7.6403E-5
92845 6.7271E-4
7100  2.3185E-3
8100  3.7473E-2
1102  5.8854E-2
MIX=2
26100 5.9088E-2
24100 1.6532E-2
28100 8.1369E-3
25100 1.3039E-3
14100 1.3603E-3
22100 5.9844E-4
END MIXT
READ GEOMETRY
HEMISPHERE 1 1 32.9537 CHORD 16.4073
SPHERE 0 1 32.9537
SPHERE 2 1 33.1037
END GEOMETRY
END DATA
```

KENO-5A Input Listing for Case 2 of Table 13.b (16-Energy-Group Hansen-Roach Cross Sections).

```
LEU-SOL-THERM-003-2
READ PARAMETERS
LIB=41
TME=360
GEN=410
NPG=2500
NSK=10
END PARAMETERS
READ MIXT
MIX=1
92400 6.0186E-7
92500 6.8143E-5
92845 4.1999E-4 92846 1.7999E-4
7100  2.0540E-3
8100  3.7042E-2
1102  5.9802E-2
MIX=2
26100 5.9088E-2
24100 1.6532E-2
28100 8.1369E-3
25100 1.3039E-3
14100 1.3603E-3
22100 5.9844E-4
END MIXT
READ GEOMETRY
HEMISPHERE 1 1 32.9537 CHORD 25.1548
SPHERE 0 1 32.9537
SPHERE 2 1 33.1037
END GEOMETRY
END DATA
```

KENO-5A Input Listing for Case 3 of Table 13.b (16-Energy-Group Hansen-Roach Cross Sections).

```
LEU-SOL-THERM-003-3
READ PARAMETERS
LIB=41
TME=360
GEN=410
NPG=2500
NSK=10
END PARAMETERS
READ MIXT
MIX=1
92400 5.9274E-7
92500 6.7111E-5
92845 3.5453E-4 92846 2.3636E-4
7100  1.9856E-3
8100  3.7040E-2
1102  6.0199E-2
MIX=2
26100 5.9088E-2
24100 1.6532E-2
28100 8.1369E-3
25100 1.3039E-3
14100 1.3603E-3
22100 5.9844E-4
END MIXT
READ GEOMETRY
SPHERE 1 1 32.9537
SPHERE 2 1 33.1037
END GEOMETRY
END DATA
```

KENO-5A Input Listing for Case 4 of Table 13.b (16-Energy-Group Hansen-Roach Cross Sections).

```
LEU-SOL-THERM-003-4
READ PARAMETERS
LIB=41
TME=360
GEN=410
NPG=2500
NSK=10
END PARAMETERS
READ MIXT
MIX=1
92400 5.8134E-7
92500 6.5820E-5
92845 3.4772E-4 92846 2.3181E-4
7100  1.9783E-3
8100  3.6939E-2
1102  6.0110E-2
MIX=2
26100 5.9088E-2
24100 1.6532E-2
28100 8.1369E-3
25100 1.3039E-3
14100 1.3603E-3
22100 5.9844E-4
END MIXT
READ GEOMETRY
HEMISPHERE 1 1 43.6303 CHORD 3.9656
SPHERE 0 1 43.6303
SPHERE 2 1 43.8203
END GEOMETRY
END DATA
```

KENO-5A Input Listing for Case 5 of Table 13.b (16-Energy-Group Hansen-Roach Cross Sections).

```
LEU-SOL-THERM-003-5
READ PARAMETERS
LIB=41
TME=360
GEN=410
NPG=2500
NSK=10
END PARAMETERS
READ MIXT
MIX=1
92400 4.6279E-7
92500 5.2398E-5
92846 4.1522E-4 92847 0.4613E-4
7100  1.5764E-3
8100  3.6225E-2
1102  6.1483E-2
MIX=2
26100 5.9088E-2
24100 1.6532E-2
28100 8.1369E-3
25100 1.3039E-3
14100 1.3603E-3
22100 5.9844E-4
END MIXT
READ GEOMETRY
HEMISPHERE 1 1 43.6303 CHORD 28.0537
SPHERE 0 1 43.6303
SPHERE 2 1 43.8203
END GEOMETRY
END DATA
```

KENO-5A Input Listing for Case 6 of Table 13.b (16-Energy-Group Hansen-Roach Cross Sections).

```
LEU-SOL-THERM-003-6
READ PARAMETERS
LIB=41
TME=360
GEN=410
NPG=2500
NSK=10
END PARAMETERS
READ MIXT
MIX=1
92400 4.4911E-7
92500 5.0849E-5
92846 3.5817E-4 92847 0.8954E-4
7100  1.5340E-3
8100  3.6175E-2
1102  6.1685E-2
MIX=2
26100 5.9088E-2
24100 1.6532E-2
28100 8.1369E-3
25100 1.3039E-3
14100 1.3603E-3
22100 5.9844E-4
END MIXT
READ GEOMETRY
SPHERE 1 1 43.6303
SPHERE 2 1 43.8203
END GEOMETRY
END DATA
```

KENO-5A Input Listing for Case 7 of Table 13.b (16-Energy-Group Hansen-Roach Cross Sections).

```
LEU-SOL-THERM-003-7
READ PARAMETERS
LIB=41
TME=360
GEN=410
NPG=2500
NSK=10
END PARAMETERS
READ MIXT
MIX=1
92400 4.3999E-7
92500 4.9817E-5
92846 3.5090E-4 92847 0.8772E-4
7100  1.5077E-3
8100  3.6117E-2
1102  6.1763E-2
MIX=2
26100 5.9088E-2
24100 1.6532E-2
28100 8.1369E-3
25100 1.3039E-3
14100 1.3603E-3
22100 5.9844E-4
END MIXT
READ GEOMETRY
HEMISPHERE 1 1 59.8897 CHORD 4.6151
SPHERE 0 1 59.8897
SPHERE 2 1 60.0997
END GEOMETRY
END DATA
```

KENO-5A Input Listing for Case 8 of Table 13.b (16-Energy-Group Hansen-Roach Cross Sections).

```
LEU-SOL-THERM-003-8
READ PARAMETERS
LIB=41
TME=360
GEN=410
NPG=2500
NSK=10
END PARAMETERS
READ MIXT
MIX=1
92400 3.8984E-7
92500 4.4138E-5
92846 1.1659E-4 92847 2.7203E-4
7100  1.3661E-3
8100  3.5868E-2
1102  6.2307E-2
MIX=2
26100 5.9088E-2
24100 1.6532E-2
28100 8.1369E-3
25100 1.3039E-3
14100 1.3603E-3
22100 5.9844E-4
END MIXT
READ GEOMETRY
HEMISPHERE 1 1 59.8897 CHORD 41.9340
SPHERE 0 1 59.8897
SPHERE 2 1 60.0997
END GEOMETRY
END DATA
```

KENO-5A Input Listing for Case 9 of Table 13.b (16-Energy-Group Hansen-Roach Cross Sections).

```
LEU-SOL-THERM-003-9
READ PARAMETERS
LIB=41
TME=360
GEN=410
NPG=2500
NSK=10
END PARAMETERS
READ MIXT
MIX=1
92400 3.8300E-7
92500 4.3364E-5
92846 1.1454E-4 92847 2.6727E-4
7100  1.3569E-3
8100  3.5837E-2
1102  6.2336E-2
MIX=2
26100 5.9088E-2
24100 1.6532E-2
28100 8.1369E-3
25100 1.3039E-3
14100 1.3603E-3
22100 5.9844E-4
END MIXT
READ GEOMETRY
SPHERE 1 1 59.8897
SPHERE 2 1 60.0997
END GEOMETRY
END DATA
```

KENO-5A Input Listing for Case 1 of Table 13.b (27-Energy-Group ENDF/B-IV Cross Sections).

```
=csas25
leu-sol-therm-003-1
27groupndf4 infhommedium
u-234 1 0 6.7481e-7 end
u-235 1 0 7.6403e-5 end
u-238 1 0 6.7271e-4 end
n     1 0 2.3185e-3 end
o     1 0 3.7473e-2 end
h     1 0 5.8854e-2 end
fe    2 0 5.9088e-2 end
cr    2 0 1.6532e-2 end
ni    2 0 8.1369e-3 end
mn    2 0 1.3039e-3 end
si    2 0 1.3603e-3 end
ti    2 0 5.9844e-4 end
end comp
leu-sol-therm-003-1
read parameters
tme=360
gen=410
npg=2500
nsk=10
end parameters
read geometry
hemisphere 1 1 32.9537 chord 16.4073
sphere 0 1 32.9537
sphere 2 1 33.1037
end geometry
end data
end
```

KENO-5A Input Listing for Case 2 of Table 13.b (27-Energy-Group ENDF/B-IV Cross Sections).

```
=csas25
leu-sol-therm-003-2
27groupndf4 infhommedium
u-234 1 0 6.0186e-7 end
u-235 1 0 6.8143e-5 end
u-238 1 0 5.9998e-4 end
n     1 0 2.0540e-3 end
o     1 0 3.7042e-2 end
h     1 0 5.9802e-2 end
fe    2 0 5.9088e-2 end
cr    2 0 1.6532e-2 end
ni    2 0 8.1369e-3 end
mn    2 0 1.3039e-3 end
si    2 0 1.3603e-3 end
ti    2 0 5.9844e-4 end
end comp
leu-sol-therm-003-2
read parameters
tme=360
gen=410
npg=2500
nsk=10
end parameters
read geometry
hemisphere 1 1 32.9537 chord 25.1548
sphere 0 1 32.9537
sphere 2 1 33.1037
end geometry
end data
end
```

KENO-5A Input Listing for Case 3 of Table 13.b (27-Energy-Group ENDF/B-IV Cross Sections).

```
=csas25
leu-sol-therm-003-3
27groupndf4 infhommedium
u-234 1 0 5.9274e-7 end
u-235 1 0 6.7111e-5 end
u-238 1 0 5.9089e-4 end
n     1 0 1.9856e-3 end
o     1 0 3.7040e-2 end
h     1 0 6.0199e-2 end
fe    2 0 5.9088e-2 end
cr    2 0 1.6532e-2 end
ni    2 0 8.1369e-3 end
mn    2 0 1.3039e-3 end
si    2 0 1.3603e-3 end
ti    2 0 5.9844e-4 end
end comp
leu-sol-therm-003-3
read parameters
tme=360
gen=410
npg=2500
nsk=10
end parameters
read geometry
sphere 1 1 32.9537
sphere 2 1 33.1037
end geometry
end data
end
```

KENO-5A Input Listing for Case 4 of Table 13.b (27-Energy-Group ENDF/B-IV Cross Sections).

```
=csas25
leu-sol-therm-003-4
27groupndf4 infhommedium
u-234 1 0 5.8134e-7 end
u-235 1 0 6.5820e-5 end
u-238 1 0 5.7953e-4 end
n     1 0 1.9783e-3 end
o     1 0 3.6939e-2 end
h     1 0 6.0110e-2 end
fe    2 0 5.9088e-2 end
cr    2 0 1.6532e-2 end
ni    2 0 8.1369e-3 end
mn    2 0 1.3039e-3 end
si    2 0 1.3603e-3 end
ti    2 0 5.9844e-4 end
end comp
leu-sol-therm-003-4
read parameters
tme=360
gen=410
npg=2500
nsk=10
end parameters
read geometry
hemisphere 1 1 43.6303 chord 3.9656
sphere 0 1 43.6303
sphere 2 1 43.8203
end geometry
end data
end
```

KENO-5A Input Listing for Case 5 of Table 13.b (27-Energy-Group ENDF/B-IV Cross Sections).

```
=csas25
leu-sol-therm-003-5
27groupndf4 infhommedium
u-234 1 0 4.6279e-7 end
u-235 1 0 5.2398e-5 end
u-238 1 0 4.6135e-4 end
n     1 0 1.5764e-3 end
o     1 0 3.6225e-2 end
h     1 0 6.1483e-2 end
fe    2 0 5.9088e-2 end
cr    2 0 1.6532e-2 end
ni    2 0 8.1369e-3 end
mn    2 0 1.3039e-3 end
si    2 0 1.3603e-3 end
ti    2 0 5.9844e-4 end
end comp
leu-sol-therm-003-5
read parameters
tme=360
gen=410
npg=2500
nsk=10
end parameters
read geometry
hemisphere 1 1 43.6303 chord 28.0537
sphere 0 1 43.6303
sphere 2 1 43.8203
end geometry
end data
end
```

KENO-5A Input Listing for Case 6 of Table 13.b (27-Energy-Group ENDF/B-IV Cross Sections).

```
=csas25
leu-sol-therm-003-6
27groupndf4 infhommedium
u-234 1 0 4.4911e-7 end
u-235 1 0 5.0849e-5 end
u-238 1 0 4.4771e-4 end
n     1 0 1.5340e-3 end
o     1 0 3.6175e-2 end
h     1 0 6.1685e-2 end
fe    2 0 5.9088e-2 end
cr    2 0 1.6532e-2 end
ni    2 0 8.1369e-3 end
mn    2 0 1.3039e-3 end
si    2 0 1.3603e-3 end
ti    2 0 5.9844e-4 end
end comp
leu-sol-therm-003-6
read parameters
tme=360
gen=410
npg=2500
nsk=10
end parameters
read geometry
sphere 1 1 43.6303
sphere 2 1 43.8203
end geometry
end data
end
```

KENO-5A Input Listing for Case 7 of Table 13.b (27-Energy-Group ENDF/B-IV Cross Sections).

```
=csas25
leu-sol-therm-003-7
27groupndf4 infhommedium
u-234 1 0 4.3999e-7 end
u-235 1 0 4.9817e-5 end
u-238 1 0 4.3862e-4 end
n     1 0 1.5077e-3 end
o     1 0 3.6117e-2 end
h     1 0 6.1763e-2 end
fe    2 0 5.9088e-2 end
cr    2 0 1.6532e-2 end
ni    2 0 8.1369e-3 end
mn    2 0 1.3039e-3 end
si    2 0 1.3603e-3 end
ti    2 0 5.9844e-4 end
end comp
leu-sol-therm-003-7
read parameters
tme=360
gen=410
npg=2500
nsk=10
end parameters
read geometry
hemisphere 1 1 59.8897 chord 4.6151
sphere 0 1 59.8897
sphere 2 1 60.0997
end geometry
end data
end
```

KENO-5A Input Listing for Case 8 of Table 13.b (27-Energy-Group ENDF/B-IV Cross Sections).

```
=csas25
leu-sol-therm-003-8
27groupndf4 infhommedium
u-234 1 0 3.8984e-7 end
u-235 1 0 4.4138e-5 end
u-238 1 0 3.8862e-4 end
n     1 0 1.3661e-3 end
o     1 0 3.5868e-2 end
h     1 0 6.2307e-2 end
fe    2 0 5.9088e-2 end
cr    2 0 1.6532e-2 end
ni    2 0 8.1369e-3 end
mn    2 0 1.3039e-3 end
si    2 0 1.3603e-3 end
ti    2 0 5.9844e-4 end
end comp
leu-sol-therm-003-8
read parameters
tme=360
gen=410
npg=2500
nsk=10
end parameters
read geometry
hemisphere 1 1 59.8897 chord 41.9340
sphere 0 1 59.8897
sphere 2 1 60.0997
end geometry
end data
end
```

KENO-5A Input Listing for Case 9 of Table 13.b (27-Energy-Group ENDF/B-IV Cross Sections).

```
=csas25
leu-sol-therm-003-9
27groupndf4 infhommedium
u-234 1 0 3.8300e-7 end
u-235 1 0 4.3364e-5 end
u-238 1 0 3.8181e-4 end
n     1 0 1.3569e-3 end
o     1 0 3.5837e-2 end
h     1 0 6.2336e-2 end
fe    2 0 5.9088e-2 end
cr    2 0 1.6532e-2 end
ni    2 0 8.1369e-3 end
mn    2 0 1.3039e-3 end
si    2 0 1.3603e-3 end
ti    2 0 5.9844e-4 end
end comp
leu-sol-therm-003-9
read parameters
tme=360
gen=410
npg=2500
nsk=10
end parameters
read geometry
sphere 1 1 59.8897
sphere 2 1 60.0997
end geometry
end data
end
```

A.4 MCNP Input Listings

The MCNP4A calculations with continuous energy ENDF/B-V cross sections were run with 1,510 generations of 2000 histories per generation and the first 10 generations skipped for a total of 3,000,000 active histories.

MCNP Input Listing for Case 1 of Table 13.b.

```
LEU-SOL-THERM-003. Case 1.
   1  1 9.939529E-02  -1 -3 imp:n=1
   2  2 8.701954E-02  1 -2 imp:n=1
   3  0 -1 3 imp:n=1
   4  0 2 imp:n=0

   1  so 32.9537
   2  so 33.1037
   3  pz 16.4073

  m1  92234.50c  6.7481E-7
      92235.50c  7.6403E-5
      92238.50c  6.7271E-4
       7014.50c  2.3185E-3
       8016.50c  3.7473E-2
       1001.50c  5.8854E-2
  m2  26000.50c  5.9088E-2
      24000.50c  1.6532E-2
      28000.50c  8.1369E-3
      25055.50c  1.3039E-3
      14000.50c  1.3603E-3
      22000.50c  5.9844E-4
 mt1   lwtr.01t
kcode  2000 1.0 10 1510
 sdef  pos=0 0 0 rad=d1 cel=1
  si1  0 32.96
prdmp  3j 1
print
```

MCNP Input Listing for Case 2 of Table 13.b.

```
LEU-SOL-THERM-003. Case 2.
   1  1 9.956672E-02  -1 -3 imp:n=1
   2  2 8.701954E-02  1 -2 imp:n=1
   3  0 -1 3 imp:n=1
   4  0 2 imp:n=0

   1  so 32.9537
   2  so 33.1037
   3  pz 25.1548

  m1  92234.50c  6.0186E-7
      92235.50c  6.8143E-5
      92238.50c  5.9998E-4
       7014.50c  2.0540E-3
       8016.50c  3.7042E-2
       1001.50c  5.9802E-2
  m2  26000.50c  5.9088E-2
      24000.50c  1.6532E-2
      28000.50c  8.1369E-3
      25055.50c  1.3039E-3
      14000.50c  1.3603E-3
      22000.50c  5.9844E-4
 mt1   lwtr.01t
kcode  2000 1.0 10 1510
 sdef  pos=0 0 0 rad=d1 cel=1
  si1  0 32.96
prdmp  3j 1
print
```

MCNP Input Listing for Case 3 of Table 13.b.

```
LEU-SOL-THERM-003. Case 3.
   1  1 9.988319E-02  -1 imp:n=1
   2  2 8.701954E-02  1 -2 imp:n=1
   3  0 2 imp:n=0

   1  so 32.9537
   2  so 33.1037

  m1  92234.50c  5.9274E-7
      92235.50c  6.7111E-5
      92238.50c  5.9089E-4
       7014.50c  1.9856E-3
       8016.50c  3.7040E-2
       1001.50c  6.0199E-2
  m2  26000.50c  5.9088E-2
      24000.50c  1.6532E-2
      28000.50c  8.1369E-3
      25055.50c  1.3039E-3
      14000.50c  1.3603E-3
      22000.50c  5.9844E-4
 mt1   lwtr.01t
kcode  2000 1.0 10 1510
 sdef  pos=0 0 0 rad=d1 cel=1
  si1  0 32.96
prdmp  3j 1
print
```

MCNP Input Listing for Case 4 of Table 13.b.

```
LEU-SOL-THERM-003. Case 4.
   1  1 9.967323E-02  -1 -3 imp:n=1
   2  2 8.701954E-02  1 -2 imp:n=1
   3  0 -1 3 imp:n=1
   4  0 2 imp:n=0

   1  so 43.6303
   2  so 43.8203
   3  pz  3.9656

  m1  92234.50c  5.8134E-7
      92235.50c  6.5820E-5
      92238.50c  5.7953E-4
       7014.50c  1.9783E-3
       8016.50c  3.6939E-2
       1001.50c  6.0110E-2
  m2  26000.50c  5.9088E-2
      24000.50c  1.6532E-2
      28000.50c  8.1369E-3
      25055.50c  1.3039E-3
      14000.50c  1.3603E-3
      22000.50c  5.9844E-4
 mt1   lwtr.01t
kcode  2000 1.0 10 1510
 sdef  pos=0 0 0 rad=d1 cel=1
  si1  0 43.64
prdmp  3j 1
print
```

MCNP Input Listing for Case 5 of Table 13.b.

```
LEU-SOL-THERM-003. Case 5.
   1  1 9.979861E-02  -1 -3 imp:n=1
   2  2 8.701954E-02  1 -2 imp:n=1
   3  0 -1 3 imp:n=1
   4  0 2 imp:n=0

   1  so 43.6303
   2  so 43.8203
   3  pz 28.0537

   m1  92234.50c  4.6279E-7
       92235.50c  5.2398E-5
       92238.50c  4.6135E-4
        7014.50c  1.5764E-3
        8016.50c  3.6225E-2
        1001.50c  6.1483E-2
   m2  26000.50c  5.9088E-2
       24000.50c  1.6532E-2
       28000.50c  8.1369E-3
       25055.50c  1.3039E-3
       14000.50c  1.3603E-3
       22000.50c  5.9844E-4
  mt1   lwtr.01t
kcode  2000 1.0 10 1510
 sdef  pos=0 0 0 rad=d1 cel=1
  si1  0 43.64
prdmp  3j 1
print
```

MCNP Input Listing for Case 6 of Table 13.b.

```
LEU-SOL-THERM-003. Case 6.
   1  1 9.989301E-02  -1 imp:n=1
   2  2 8.701954E-02  1 -2 imp:n=1
   3  0 2 imp:n=0

   1  so 43.6303
   2  so 43.8203

  m1  92234.50c  4.4911E-7
      92235.50c  5.0849E-5
      92238.50c  4.4771E-4
       7014.50c  1.5340E-3
       8016.50c  3.6175E-2
       1001.50c  6.1685E-2
  m2  26000.50c  5.9088E-2
      24000.50c  1.6532E-2
      28000.50c  8.1369E-3
      25055.50c  1.3039E-3
      14000.50c  1.3603E-3
      22000.50c  5.9844E-4
 mt1   lwtr.01t
kcode  2000 1.0 10 1510
 sdef  pos=0 0 0 rad=d1 cel=1
  si1  0 43.64
prdmp  3j 1
print
```

MCNP Input Listing for Case 7 of Table 13.b.

```
LEU-SOL-THERM-003. Case 7.
   1  1 9.987658E-02  -1 -3 imp:n=1
   2  2 8.701954E-02  1 -2 imp:n=1
   3  0 -1 3 imp:n=1
   4  0 2 imp:n=0

   1  so 59.8897
   2  so 60.0997
   3  pz  4.6151

  m1  92234.50c  4.3999E-7
      92235.50c  4.9817E-5
      92238.50c  4.3862E-4
       7014.50c  1.5077E-3
       8016.50c  3.6117E-2
       1001.50c  6.1763E-2
  m2  26000.50c  5.9088E-2
      24000.50c  1.6532E-2
      28000.50c  8.1369E-3
      25055.50c  1.3039E-3
      14000.50c  1.3603E-3
      22000.50c  5.9844E-4
 mt1   lwtr.01t
kcode  2000 1.0 10 1510
 sdef  pos=0 0 0 rad=d1 cel=1
  si1  0 59.89
prdmp  3j 1
print
```

MCNP Input Listing for Case 8 of Table 13.b.

```
LEU-SOL-THERM-003. Case 8.
   1  1 9.997425E-02  -1 -3 imp:n=1
   2  2 8.701954E-02  1 -2 imp:n=1
   3  0 -1 3 imp:n=1
   4  0 2 imp:n=0

   1  so 59.8897
   2  so 60.0997
   3  pz 41.9340

   m1  92234.50c  3.8984E-7
       92235.50c  4.4138E-5
       92238.50c  3.8862E-4
        7014.50c  1.3661E-3
        8016.50c  3.5868E-2
        1001.50c  6.2307E-2
   m2  26000.50c  5.9088E-2
       24000.50c  1.6532E-2
       28000.50c  8.1369E-3
       25055.50c  1.3039E-3
       14000.50c  1.3603E-3
       22000.50c  5.9844E-4
  mt1   lwtr.01t
kcode  2000 1.0 10 1510
 sdef  pos=0 0 0 rad=d1 cel=1
  si1  0 59.89
prdmp  3j 1
print
```

MCNP Input Listing for Case 9 of Table 13.b.

```
LEU-SOL-THERM-003. Case 9.
   1  1 9.995546E-02  -1 imp:n=1
   2  2 8.701954E-02  1 -2 imp:n=1
   3  0 2 imp:n=0

   1  so 59.8897
   2  so 60.0997

  m1  92234.50c  3.8300E-7
      92235.50c  4.3364E-5
      92238.50c  3.8181E-4
       7014.50c  1.3569E-3
       8016.50c  3.5837E-2
       1001.50c  6.2336E-2
  m2  26000.50c  5.9088E-2
      24000.50c  1.6532E-2
      28000.50c  8.1369E-3
      25055.50c  1.3039E-3
      14000.50c  1.3603E-3
      22000.50c  5.9844E-4
 mt1   lwtr.01t
kcode  2000 1.0 10 1510
 sdef  pos=0 0 0 rad=d1 cel=1
  si1  0 59.89
prdmp  3j 1
print
```

A.5 ONEDANT Input Listings

The inputs given below for the Case 3, Case 6, and Case 9 are for the ONEDANT code using the 27-group ENDF/B-IV cross sections created by CSASI of the ORNL SCALE4.3 code system. P_3S_{16} calculations were performed using the default value for convergence (epsi) = 0.0001. The problems were run with 100 mesh points in the core and 10 meshes in the stainless steel shell.

CSASI Input for Cross Section Preparation used in ONEDANT Calculations for Case 3 of Table 13.b.

```
=csasi
leu-sol-therm-003-3
27groupndf4 infhommedium
u-234 1 0 5.9274e-7 end
u-235 1 0 6.7111e-5 end
u-238 1 0 5.9089e-4 end
n     1 0 1.9856e-3 end
o     1 0 3.7040e-2 end
h     1 0 6.0199e-2 end
fe    2 0 5.9088e-2 end
cr    2 0 1.6532e-2 end
ni    2 0 8.1369e-3 end
mn    2 0 1.3039e-3 end
si    2 0 1.3603e-3 end
ti    2 0 5.9844e-4 end
end comp
end
```

ONEDANT Input for Case 3 of Table 13.b.

```
     1
  LEU-SOL-THERM-003, Case 3
/ * * *  block   I  * * *
 igeom=sph
 ngroup=27
 isn=16
 niso=2
 mt=2
 nzone=2
 im=2
 it=110
   t
/ * * *  block  II  * * *
 xmesh= 0. 32.9537 33.1037
 xints= 100 10
 zones= 1 2
   t
/ * * *  block III  * * *
 lib=xslib3
 maxord=3
 ihm=42
 iht=3
 ihs=16
 ititl=1
 ifido=0
 i2lp1=1
 chivec=.021 .188 .215 .125 .166 .180 .090 .014 .001 18z
   t
/ * * *  block  IV  * * *
 matls= isos
 assign=matls
   t
/ * * *  block   V  * * *
 ievt=1
 isct=3
 ith=0
 ibr=0
   t
```

CSASI Input for Cross Section Preparation used in ONEDANT Calculations for Case 6 of Table 13.b.

```
=csasi
leu-sol-therm-003-6
27groupndf4 infhommedium
u-234 1 0 4.4911e-7 end
u-235 1 0 5.0849e-5 end
u-238 1 0 4.4771e-4 end
n     1 0 1.5340e-3 end
o     1 0 3.6175e-2 end
h     1 0 6.1685e-2 end
fe    2 0 5.9088e-2 end
cr    2 0 1.6532e-2 end
ni    2 0 8.1369e-3 end
mn    2 0 1.3039e-3 end
si    2 0 1.3603e-3 end
ti    2 0 5.9844e-4 end
end comp
end
```

ONEDANT Input for Case 6 of Table 13.b.

```
    1
  LEU-SOL-THERM-003, Case 6
/ * * *  block   I  * * *
 igeom=sph
 ngroup=27
 isn=16
 niso=2
 mt=2
 nzone=2
 im=2
 it=110
   t
/ * * *  block  II  * * *
 xmesh= 0. 43.6303 43.8203
 xints= 100 10
 zones= 1 2
   t
/ * * *  block III  * * *
 lib=xslib6
 maxord=3
 ihm=42
 iht=3
 ihs=16
 ititl=1
 ifido=0
 i2lp1=1
 chivec=.021 .188 .215 .125 .166 .180 .090 .014 .001 18z
   t
/ * * *  block  IV  * * *
 matls= isos
 assign=matls
   t
/ * * *  block   V  * * *
 ievt=1
 isct=3
 ith=0
 ibr=0
   t
```

CSASI Input for Cross Section Preparation used in ONEDANT Calculations for Case 9 of Table 13.b.

```
=csasi
leu-sol-therm-003-9
27groupndf4 infhommedium
u-234 1 0 3.8300e-7 end
u-235 1 0 4.3364e-5 end
u-238 1 0 3.8181e-4 end
n     1 0 1.3569e-3 end
o     1 0 3.5837e-2 end
h     1 0 6.2336e-2 end
fe    2 0 5.9088e-2 end
cr    2 0 1.6532e-2 end
ni    2 0 8.1369e-3 end
mn    2 0 1.3039e-3 end
si    2 0 1.3603e-3 end
ti    2 0 5.9844e-4 end
end comp
end
```

ONEDANT Input for Case 9 of Table 13.b.

```
    1
  LEU-SOL-THERM-003, Case 9
/ * * *  block   I  * * *
 igeom=sph
 ngroup=27
 isn=16
 niso=2
 mt=2
 nzone=2
 im=2
 it=110
   t
/ * * *  block  II  * * *
 xmesh= 0. 59.8897 60.0997
 xints= 100 10
 zones= 1 2
   t
/ * * *  block III  * * *
 lib=xslib9
 maxord=3
 ihm=42
 iht=3
 ihs=16
 ititl=1
 ifido=0
 i2lp1=1
 chivec=.021 .188 .215 .125 .166 .180 .090 .014 .001 18z
   t
/ * * *  block  IV  * * *
 matls= isos
 assign=matls
   t
/ * * *  block   V  * * *
 ievt=1
 isct=3
 ith=0
 ibr=0
   t
```

APPENDIX B: ADDITIONAL CALCULATIONAL RESULTS

Some calculations were performed using nonstandard code/cross-section set combinations. The results are shown in Table B.1.

28-Group ABBN-90 Cross Sections

The ABBN-90 multigroup cross-section set was prepared for the calculations by the CONSYST2 code. A 28-group approximation was used.

The KENO-5A calculations were run with 410 generations of 2500 histories per generation and the first 10 generations skipped for a total of 1,000,000 active histories.

The ONEDANT calculations were run with 100 mesh points in the core and 10 meshes in the stainless steel shell using the default value for convergence (epsi) = 0.0001. P_5S_{16} calculations were performed.

44-Group ENDF/B-V Cross Sections

The problems were run with the KENO-5A code with the ORNL SCALE4.3 code system using the CSAS option and the 44-group ENDF/B-V cross sections. The problems were run with 1,000,000 active and 25,000 inactive histories (400 active generations, ten skipped generations, and 2500 histories/generation).

The problems were run with the ONEDANT code using the 44-group ENDF/B-V cross sections created by CSASI of the ORNL SCALE4.3 code system. P_3S_{16} calculations were performed using the default value for convergence (epsi) = 0.0001. The problems were run with 100 mesh points in the core and 10 meshes in the stainless steel shell.

Table B.1. Additional Calculation Results.[a]

Code (Cross Section Set) → Configuration ↓	KENO (28-Group ABBN-90)	ONEDANT (28-Group ABBN-90)	KENO (44-Group ENDF/B-V)	ONEDANT (44-Group ENDF/B-V)
1	1.0060 ± 0.0007	--	0.9978 ± 0.0007	--
2	1.0047 ± 0.0006	--	0.9966 ± 0.0006	--
3	1.0085 ± 0.0006	1.0090	1.0027 ± 0.0007	1.0034
4	1.0031 ± 0.0007	--	0.9941 ± 0.0007	--
5	1.0056 ± 0.0005	--	0.9975 ± 0.0005	--
6	1.0052 ± 0.0005	1.0048	0.9975 ± 0.0005	0.9991
7	1.0040 ± 0.0005	--	0.9970 ± 0.0005	--
8	1.0061 ± 0.0005	--	0.9985 ± 0.0005	--
9	1.0020 ± 0.0005	1.0027	0.9987 ± 0.0004	0.9930

(a) Results supplied by authors.